

The formation number of vortex rings formed in uniform background co-flow

By PAUL S. KRUEGER¹, JOHN O. DABIRI²
AND MORTEZA GHARIB²

¹Department of Mechanical Engineering, Southern Methodist University,
PO Box 750 337, Dallas, TX 75275-0337, USA

²Graduate Aeronautical Laboratories and Bioengineering, California Institute of Technology,
Pasadena, CA 91125, USA

(Received 17 February 2005 and in revised form 28 October 2005)

The formation of vortex rings generated by an impulsively started jet in the presence of uniform background co-flow is studied experimentally to extend previous results. A piston–cylinder mechanism is used to generate the vortex rings and the co-flow is supplied through a transparent shroud surrounding the cylinder. Digital particle image velocimetry (DPIV) is used to measure the development of the ring vorticity and its eventual pinch off from the generating jet for ratios of the co-flow to jet velocity (R_v) in the range 0 – 0.85. The formation time scale for the ring to obtain maximal circulation and pinch off from the generating jet, called the formation number (F), is determined as a function of R_v using DPIV measurements of circulation and a generalized definition of dimensionless discharge time or ‘formation time’. Both simultaneous initiation and delayed initiation of co-flow are considered. In all cases, a sharp drop in F (taking place over a range of 0.1 in R_v) is centred around a critical velocity ratio (R_{crit}). As the initiation of co-flow was delayed, the magnitude of the drop in F and the value of R_{crit} decreased. A kinematic model based on the relative velocities of the forming ring and jet shear layer is formulated and correctly predicts vortex ring pinch off for $R_v > R_{crit}$. The results of the model indicate the reduction in F at large R_v is directly related to the increased convective velocity provided to the ring by the co-flow.

1. Introduction

The formation of vortex rings by long duration starting jets is governed primarily by the roll-up of the jet shear layer (Didden 1979). Gharib, Rambod & Shariff (1998) demonstrated a limiting process whereby the shear layer roll-up is interrupted and the forming vortex ring pinches off from the generating jet in terms of entrainment of circulation. The non-dimensional time beyond which additional circulation ejected by the jet was no longer entrained into the vortex ring was recognized as a characteristic time scale for vortex ring formation and dubbed the ‘formation number’, F . Subsequent studies have confirmed the work of Gharib *et al.*, elucidated the mechanics of the pinch off process, and proposed methods for manipulating the formation number (Rosenfeld, Rambod & Gharib 1998; Zhao, Frankel & Mongeau 2000; Mohseni, Ran & Colonius 2001). Models for predicting the formation number have also been developed (Mohseni & Gharib 1998; Shusser & Gharib 2000; Linden & Turner 2001). Much of the work in this area has been motivated by the observation

that vortex rings probably play an important role in many physical processes involving starting jets, ranging from blood flow in the human left ventricle to propulsion of various aquatic creatures. (For examples of vortex rings in natural jet propulsion see Dabiri *et al.* 2005 and Madin 1990.) The significance of vortex ring formation for propulsion was demonstrated by Krueger & Gharib (2003) who showed that the average thrust during a pulse is maximized by jet pulses of non-dimensional duration very near the formation number. This was true even if the formation number was changed by varying the jet velocity program used to generate the vortex rings.

The majority of the work in vortex ring pinch off has dealt with jets issuing into quiescent fluid. In many of the physical processes of interest, however, the ambient fluid is not quiescent and background flow must be considered. A notable example is propulsion, in which case the motion of the vehicle/organism leads to a co-flow surrounding the jet responsible for propulsion. The presence of a background co-flow will modify the jet shear layer, affecting the vortex ring roll-up and the pinch off process. Hence, co-flow could significantly affect propulsive performance and its effect should be considered an integral part of the propulsive mechanism.

The effect of co-flow on vortex ring formation and pinch off has been highlighted in recent preliminary studies. Dabiri & Gharib (2004) demonstrated that a bulk counter-flow (ambient flow counter to the jet flow) can delay vortex ring pinch off, constituting the first experimental demonstration of a mechanism for delaying pinch off. Motivated by applications of pulsed-jets in propulsion, Krueger, Dabiri & Gharib (2003) considered the effect of uniform co-flow (ambient flow in the jet direction) initiated simultaneously with the jet. Simultaneous initiation of the flows is most relevant for propulsion of a vehicle accelerating from rest. The results demonstrated a reduction in the jet vorticity flux with increased co-flow, resulting in a reduction in the strength of the leading vortex ring. The formation number was also affected, but, at low co-flow velocities, only a gradual reduction in the formation number (from about 4 to about 3) was observed as the level of co-flow was increased. As the ratio of the co-flow velocity to the jet velocity, R_v , increased from 0.5 to 0.75, however, the formation number dropped from about 3 to below 1 and the leading vortex ring virtually disappeared. While the significance of the abrupt drop in formation number over a short range in R_v has important consequences for propulsion applications, the limited and preliminary nature of the data prevented a detailed analysis of the mechanism leading to the rapid reduction in formation number as R_v was increased.

The focus of the present investigation is to investigate in detail the sudden drop in formation number at large R_v observed by Krueger *et al.* (2003). To this end, pinch off is investigated in the presence of co-flow for a greater number of velocity ratios to resolve better the location and nature of the drop in formation number. In addition, the present study is not restricted to simultaneous flow initiation; cases with delayed initiation of the co-flow are also considered. Finally, a physical mechanism for the rapid reduction in the formation number and premature termination of the vortex ring formation at large co-flow values will be presented.

2. Experimental set-up

Vortex ring formation and pinch off was studied experimentally in water using a piston-cylinder vortex ring generator with co-flow supplied through a concentric shroud. A diagram of the apparatus is shown in figure 1. A constant-head tank supplied flow to the vortex ring generator while an independent pump supplied the co-flow. Separate solenoid valves, actuated by a computer, controlled the initiation

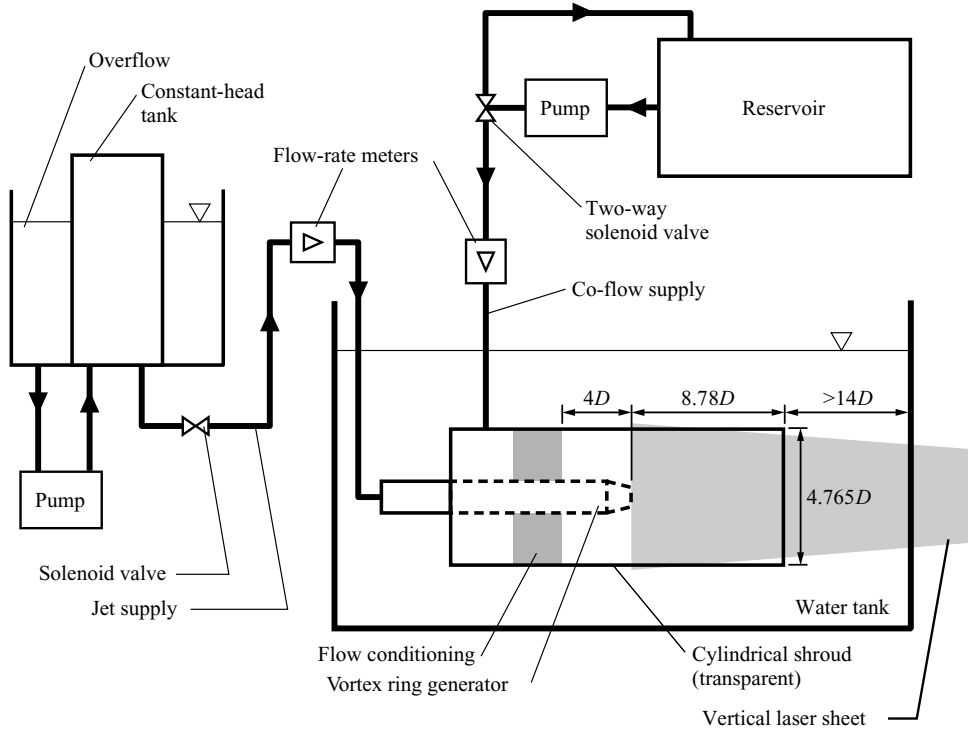


FIGURE 1. Schematic of the experimental set-up. The nozzle diameter is $D = 2.54$ cm.

of each flow, allowing independent actuation of the jet and co-flow velocities. The flow rates were measured using Transonic Systems T-110 ultrasonic flow-rate sensors, providing measurements of the time-varying piston and co-flow velocities $U_p(t)$ and $V_c(t)$, respectively.

A detailed view of the vortex ring generator near the nozzle exit plane, as well as the coordinate system used in this investigation, is shown in figure 2. The vortex ring generator used a piston with diameter $D = 2.54$ cm and had a wedge tip angle of 7° to prevent separation of the co-flow as it approached the nozzle exit plane. The shroud supplying the co-flow was made of transparent Plexiglas to allow for direct visualization of the vortex ring formation process. The shroud had negligible influence on vortex ring formation and pinch off. For instance, flow visualization of ring formation with and without the shroud in place showed that during the roll-up process, the vortex ring velocity was unaffected by the shroud (to within experimental uncertainty) and the ring diameter was altered by less than 5%. Additionally, as will be shown later, the formation number for no co-flow was unaffected by the shroud.

Digital particle image velocimetry (DPIV) was used to measure the velocity field and azimuthal vorticity downstream of the nozzle ($x > 0$). The flow was seeded with $20 \mu\text{m}$, neutrally buoyant silver-coated hollow glass spheres. The particles were illuminated with a pulsed Nd:YAG laser and imaged through the shroud with a UNIQ Vision UP – 1830 CCD camera at 30 f.p.s. and a resolution of 1024×1024 pixels. The tank in figure 1 is shown from the perspective of the camera and the light sheet from the laser illuminated the flow through the front of the shroud as shown. The particle images were processed to obtain the velocity field data according to the method developed

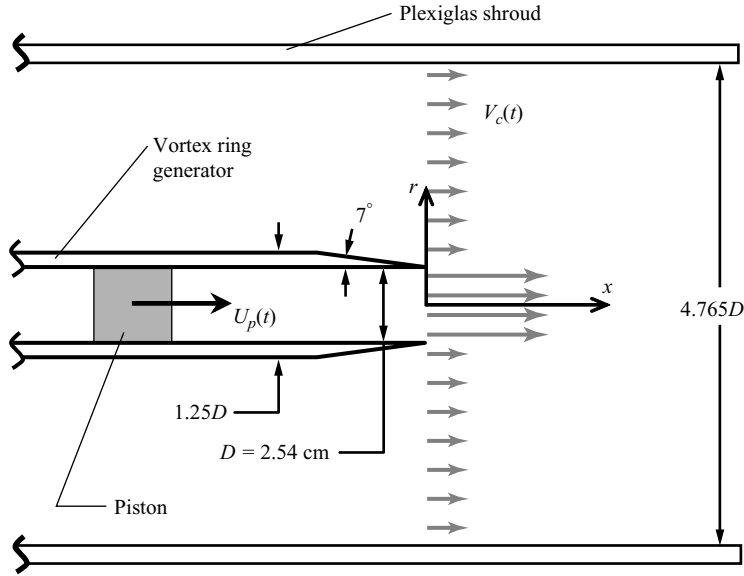


FIGURE 2. Detail of the vortex ring generator near the nozzle exit plane.

by Willert & Gharib (1991) combined with a window-shifting algorithm (Westerweel, Dabiri & Gharib 1997) for improved accuracy. The interrogation window used in the image processing was 32×32 pixels with 50% overlap. For the image magnification used with the majority of the cases, this provided velocity fields with a vector spacing of $0.09D \times 0.09D$ in the region $\{0 \leq x/D \leq 5.45, 0 \leq r/D \leq 2.38\}$ where $r/D = 2.38$ is the edge of the shroud. For several cases at low co-flow velocity, a wider view was required to capture the entire pinch off process. In these cases, the processed data provided vector spacing of $0.13D \times 0.13D$ in the region $\{0 \leq x/D \leq 7.89, 0 \leq r/D \leq 2.38\}$. Both resolutions were sufficient to distinguish the vortex roll-up and pinch off.

The average uncertainty in the particle displacements determined using the DPIV algorithm with window shifting was 0.04 pixels (Westerweel *et al.* 1997). The time delay between images was adjusted so that the maximum particle displacement (located on the jet centreline at the nozzle exit plane) was 7–8 pixels, giving an uncertainty better than 1% for the majority of the data. The exception was the data outside the jet for $R_v = 0$. For the image resolutions and time delays used in the experiments, the 0.04 pixel uncertainty translates into a physical uncertainty of 0.04 cm s^{-1} . This accounts for uncertainties with the imaging technique and algorithm (such as low seeding density and particle-size effects). Accounting for optical distortions and other sources of error, we estimate that the uncertainty in the velocity data was less than 0.1 cm s^{-1} . Vorticity was computed using finite differences of the velocity data at eight neighbouring points in a second-order accurate scheme. The uncertainty in the vorticity data was within 0.23 s^{-1} , which was less than 3% of the smallest peak vorticity observed in any of the vortex rings.

The velocity programs for the piston and co-flow velocities consisted of a rapid ramp up to steady-state values of U_0 and V_0 , respectively. The flows were maintained at their steady-state values long enough to observe vortex ring pinch off, and the co-flow was terminated last. An example of a typical run is shown in figure 3 for a

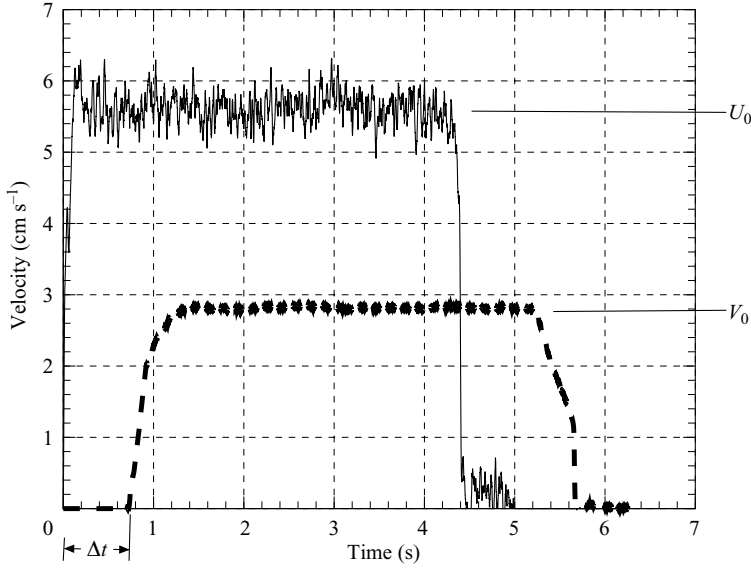


FIGURE 3. Typical piston and co-flow velocity programs. The case shown is $R_v = 0.50$, $\Delta\hat{t} = 1.54$. —, U_p ; ---, V_c .

velocity ratio of $R_v = 0.50$ and a Reynolds number of $Re_s = 640$ where

$$R_v \equiv \frac{V_0}{U_0} \quad (1)$$

and

$$Re_s \equiv \frac{|U_0 - V_0| D}{\nu} = Re_j |1 - R_v|. \quad (2)$$

Re_s is the Reynolds number based on the shear-layer strength (at steady state) and Re_j is the steady-state jet Reynolds number, namely $U_0 D / \nu$. As illustrated in figure 3, initiation of the jet and co-flow may be offset by a time interval Δt . The example in figure 3 corresponds to $\Delta t = 0.73$ s or, in dimensionless form, $\Delta\hat{t} = 1.54$ where

$$\Delta\hat{t} \equiv \frac{\Delta t (\overline{U}_p)}{D}, \quad (3)$$

and \overline{U}_p is the running average of the piston velocity. Physically, $\Delta\hat{t}$ is the piston displacement achieved before the co-flow is initiated. In this study, only cases with $\Delta\hat{t} \geq 0$ (jet initiated first) are considered. It should be noted that, owing to the unsteady initiation of the flow, the addition of co-flow is not equivalent to no co-flow with a Galilean transformation of the jet velocity to $U_p(t) - V_0$, even for $\Delta\hat{t} = 0$.

A representative cross-section of the actual jet and co-flow velocity profile obtained from DPIV is shown in figure 4. The data is plotted in a Cartesian plane to illustrate the symmetry of the flow. In this case, $\pm y$ represent radial locations in the $\theta = 0$ and π planes, respectively. The cross-section is taken at $x/D = 0.07$ for $U_0 = 5.61$ cm s⁻¹, $R_v = 0.45$, $\Delta\hat{t} = 0$, and $t = 0.93$ s (well after the startup transients were completed). This close to the nozzle exit there is a wake between the jet and co-flow at $|y|/D = 0.50$. The decrease in velocity as $|y|/D \rightarrow 2.38$ is from the boundary layer on the shroud. Outside of the boundary-layer regions, the co-flow is very nearly uniform. For all of the cases considered, the co-flow was uniform to within 0.25 cm s⁻¹ outside of

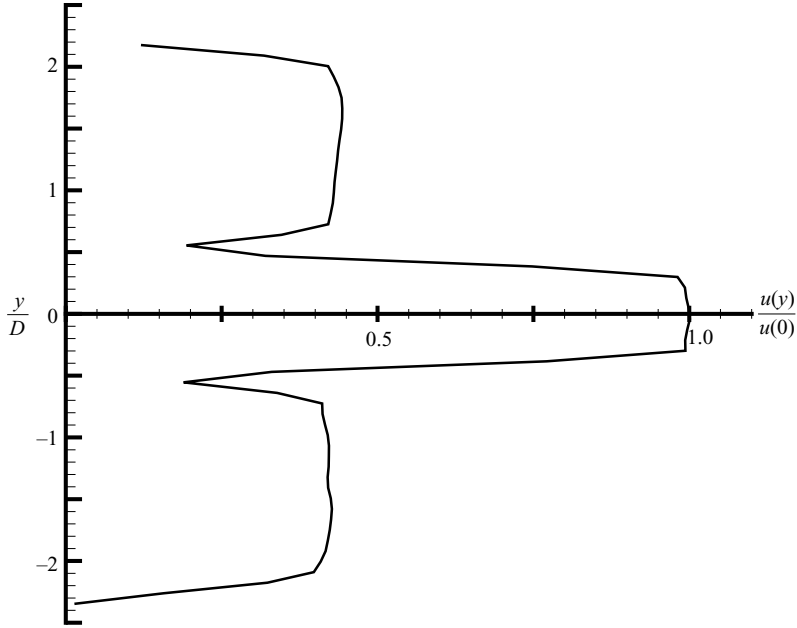


FIGURE 4. A representative cross-section of the jet and co-flow velocities. The conditions are $x/D = 0.07$, $U_0 = 5.61 \text{ cm s}^{-1}$, $R_v = 0.45$, $\Delta \hat{t} = 0$ and $t = 0.93 \text{ s}$. The data are plotted in a Cartesian plane with $\pm y$ representing radial locations in the $\theta = 0$ and π planes, respectively.

Re_j	$\Delta \hat{t}$	R_v (nominal [†])
1270 ± 12	0	0, 0.25, 0.35–0.75 (0.05 increments), 0.85
	0.34 ± 0.02	(0), 0.25, 0.35–0.75 (0.05 increments)
	0.79 ± 0.02	(0), 0.25–0.60 (0.05 increments)
	1.53 ± 0.02	(0), 0.25–0.60 (0.05 increments)

[†]The actual velocity ratios were within 0.02 of the nominal values in all cases.

TABLE 1. Summary of co-flow conditions investigated.

the boundary layers. By definition, $U_p(t)$ and $V_c(t)$ are spatially averaged across the jet and co-flow regions, respectively. Owing to boundary-layer growth, the centreline velocity can increase noticeably above U_0 so that the ratio of the actual co-flow velocity (outside the boundary layers) to the centreline velocity decreases with time. Immediately following flow initiation, however, this ratio is within a few per cent of V_0/U_0 .

The co-flow conditions investigated are given in table 1. The $R_v = 0$ case corresponds to the no co-flow case considered by Gharib *et al.* (1998) and $\Delta \hat{t}$ is irrelevant for this velocity ratio. The lowest $\Delta \hat{t}$ corresponds to $\Delta t \approx 0.19 \text{ s}$ (nominally), which is approximately twice the ramp-up time for the jet flow. The co-flow ramp-up times varied slightly with velocity ratio, from 0.57 s for $R_v = 0.25$ to 0.27 s at $R_v = 0.85$ (the highest R_v considered). Because of the limitations of the experimental set-up, only one value of Re_j (corresponding to $U_0 = 5.59 \text{ cm s}^{-1}$, nominally) was considered.

3. Qualitative observations of vortex ring pinch off in co-flow

Figures 5, 6 and 7 illustrate the progression of vortex ring development and eventual pinch off for the cases of $R_v = 0$, 0.36 and 0.76, respectively, at $\Delta \hat{t} = 0$ (simultaneously

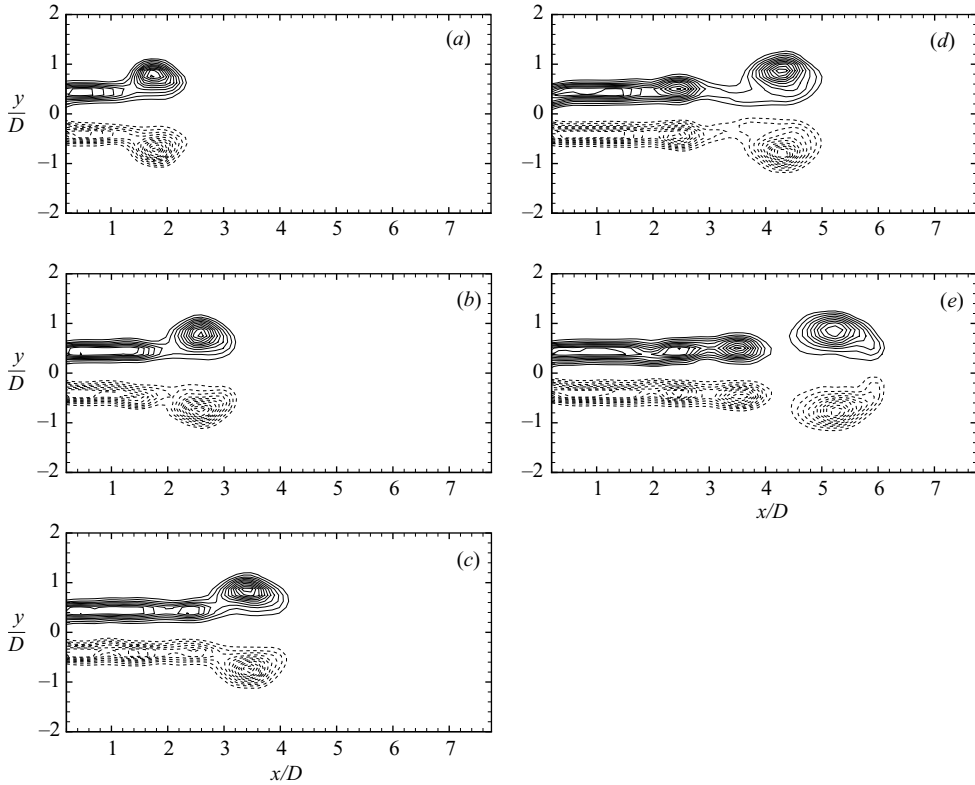


FIGURE 5. Vortex ring pinch off for $R_v=0$ and $\Delta\hat{t}=0$ at time (a) 2.07 s ($\hat{t}=4.45$), (b) 2.73 s ($\hat{t}=5.90$), (c) 3.40 s ($\hat{t}=7.36$), (d) 4.07 s ($\hat{t}=8.81$) and (e) 4.73 s ($\hat{t}=9.54$). The formation time \hat{t} is defined in equation (4). The data is plotted in a Cartesian plane with $\pm y$ representing radial locations in the $\theta=0$ and π planes, respectively. The minimum contour shown is $\omega_z D/U_0=0.91$ (of a given sense) with contour divisions of 0.45 thereafter. Dashed contours indicate negative vorticity.

initiated co-flow), as reckoned by the DPIV measurements of vorticity (ω_z). Similar to figure 4, the data are plotted in a Cartesian plane to illustrate the symmetry of the flow. The vorticity has been non-dimensionalized by U_0/D . The minimum contour (of a given sense) plotted in these figures is $\omega_z D/U_0=0.91$, with divisions of 0.45 thereafter. (The choice of the minimum contour level will be discussed in §5.) The vorticity plots indicate that the vortex ring formation was symmetric. In one trial, however, asymmetric initiation of the co-flow caused the vortex ring to tilt slightly, so the data for that trial was disregarded.

The $R_v=0$ data in figure 5 corresponds to no co-flow. For this special case, the vortex ring has a rapid initial development and soon begins convecting away from the nozzle exit plane (figure 5a). The ring continues developing, but its entrainment of circulation slows. Eventually, it entrains a significant segment of the trailing jet (figure 5c, d). The result is that the ring vorticity becomes disconnected (pinched off) from the vorticity in the generating jet and the ring stops entraining circulation (figure 5e). Figure 5 (e) also shows the development of Kelvin–Helmholtz instabilities in the jet following the ring. These observations agree qualitatively with previous studies of vortex ring pinch off in the absence of co-flow (Gharib *et al.* 1998; Rosenfeld *et al.* 1998; Zhao *et al.* 2000; Mohseni *et al.* 2001). At present, the $R_v=0$ results provide a useful comparison for the $R_v>0$ cases while illustrating the basic features of the pinch off process.

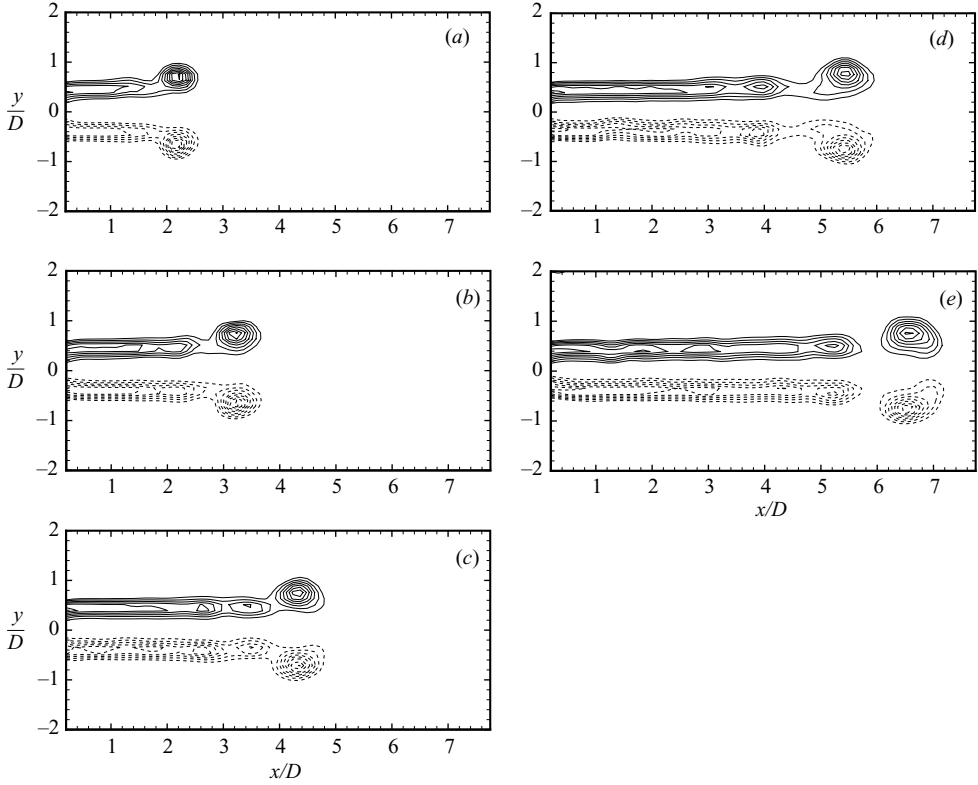


FIGURE 6. Vortex ring pinch off for $R_v = 0.36$ and $\Delta \hat{t} = 0$ at time (a) 1.67 s ($\hat{t} = 4.83$), (b) 2.33 s ($\hat{t} = 6.84$), (c) 3.00 s ($\hat{t} = 8.87$), (d) 3.67 s ($\hat{t} = 10.9$) and (e) 4.33 s ($\hat{t} = 12.9$). The contour levels are the same as in figure 5.

A case with moderate velocity ratio is shown in figure 6 ($R_v = 0.36$). The overall character of the pinch off process is similar to the $R_v = 0$ case, but some key differences are apparent. Specifically, the pinched off vortex ring is smaller and has less circulation (figure 6e). Also, the Kelvin–Helmholtz instabilities in the trailing jet are noticeably less intense, which is associated with the decreased growth rate of the instabilities as $|U_0 - V_0|$ decreases (equivalently, as $R_v \rightarrow 1$). This can be clearly seen by comparing figures 6(e) and 5(d) since the vorticity peaks in figure 6(e) have had more time to develop, but are of smaller amplitude.

A high-velocity ratio example is shown in figure 7 ($R_v = 0.76$). This case is distinctly different from the previous two. The leading vortex ring pinches off from the jet almost immediately. As a result, the ring is very weak. As the flow evolves, the separation between the ring and the jet increases. Also, as expected, instabilities in the jet have much smaller amplitude and are difficult to distinguish.

The results for $\Delta \hat{t} > 0$ are qualitatively similar to those presented above. The primary difference is that the strength of the leading vortex increases with increasing $\Delta \hat{t}$ since the vorticity flux is higher during the initial jet startup when the co-flow is off. As will be discussed below, this affects when pinch off occurs as R_v is increased.

4. Formation time

As discussed by Gharib *et al.* (1998), a key parameter describing the vortex ring formation process is the time t during which the jet shear layer has been ejecting

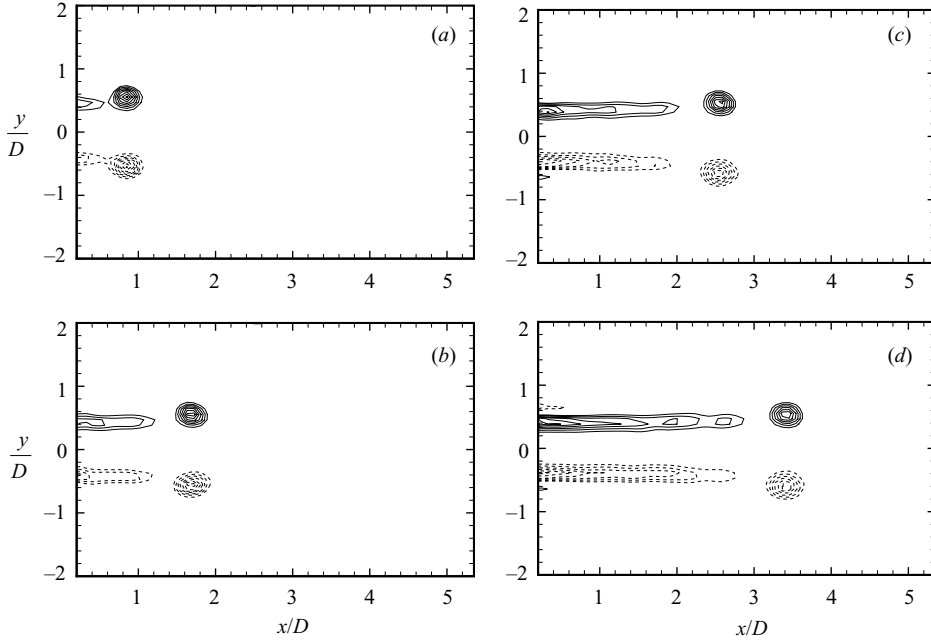


FIGURE 7. Vortex ring pinch off for $R_v = 0.76$ and $\Delta \hat{t} = 0$ at time (a) 0.53 s ($\hat{t} = 1.79$), (b) 0.93 s ($\hat{t} = 3.34$), (c) 1.33 s ($\hat{t} = 4.89$), and (d) 1.73 s ($\hat{t} = 6.44$). The contour levels are the same as in figure 5.

vorticity (the ‘discharge time’). Using the running average of the piston velocity and the nozzle diameter as appropriate velocity and length scales, they proposed the dimensionless ‘formation time’, $t \bar{U}_p / D$, as a characteristic parameter describing the formation process. Specifically, the formation time beyond which additional circulation ejected by the jet was no longer entrained by the leading vortex ring was called the ‘formation number’, F .

When co-flow is present, vortex ring formation is related not only to the jet flow, but to the jet and co-flow combination. Hence, the ‘formation time’ characterizing the formation process should include the co-flow in a physically reasonable way. Krueger *et al.* (2003) proposed generalizing formation time to

$$\hat{t} \equiv \frac{t(\bar{U}_p + \bar{V}_c)}{D}, \quad (4)$$

where \bar{V}_c is the running average of the co-flow velocity. The justification given for this choice was that the dimensionless rate of circulation provided by the apparatus (as reckoned by the slug model, see Shariff & Leonard 1992) is independent of co-flow, at least in the case of impulsively started jet and co-flow. Since then, Dabiri & Gharib (2004) have demonstrated experimentally that equation (4) is the proper generalization of formation time for vortex ring formation in counterflow (i.e. $V_c(t) < 0$) as well.

Generalizing the formation time based on the scaling of the rate of circulation provided by the jet is a logical approach, but additional physical insight can be obtained by considering the vortex ring velocity. In the presence of co-flow, the vortex ring velocity is given by

$$W_r = W_i(t) + V_c(t), \quad (5)$$

where W_i is the self-induced velocity of the vortex ring. Specifically, W_i is determined by

$$W_i = \left(\frac{\partial E}{\partial I} \right) \Big|_{\text{fixed } \Gamma \text{ and volume}} \quad (6)$$

where I , E and Γ are, respectively, the impulse, kinetic energy and circulation added to the flow (Mohseni & Gharib 1998; Mohseni *et al.* 2001). For simplicity, we consider the case where the jet and co-flow are initiated impulsively and simultaneously (so that $U_p(t) = U_0$ and $V_c(t) = V_0$ for $t > 0$). Then using the slug model to estimate I and E gives

$$E \approx \frac{1}{2} (U_0 - V_0) I. \quad (7)$$

The velocity difference appears in this expression because the energy and impulse are evaluated in the frame of reference moving with the co-flow (since only the quantities added to the background flow are relevant for W_i). Although the slug model ignores over-pressure at the nozzle exit plane developed during the unsteady ring formation process (Gharib *et al.* 1998; Krueger 2001, 2005; Krueger & Gharib 2003), equation (7) provides a reasonable estimate of the kinetic energy supplied to the flow for large discharge times. Combining results, the ring velocity predicted by the slug model for this simplified case is

$$W_r \approx \frac{1}{2} (U_0 - V_0) + V_0 = \frac{1}{2} (U_0 + V_0). \quad (8)$$

For no co-flow, this reduces to the familiar slug-model prediction that the ring velocity is half the piston velocity.

For impulsively started piston and co-flow velocities, it is apparent that $\bar{U}_p(t) = U_0$ and $\bar{V}_c(t) = V_0$. Thus, combining equation (8) with equation (4) illustrates that the generalized formation time is related to the ring velocity, namely, $\hat{t} \approx 2t W_r / D$. The same relationship holds whether or not co-flow is present (at least for the simplified example considered here). Moreover, relating the ring velocity to the velocity scale used in the formation time is appealing physically since the ring velocity is a fundamental parameter of the ring dynamics, independent of the method used to generate the vortex ring. This observation was used by Mohseni *et al.* (2001), who defined a formation time based on the ring velocity since it is the most relevant velocity governing the final state of the pinched off vortex ring. These observations support equation (4) as the appropriate generalization of the formation time for the present investigation.

With an appropriate formation time identified, the formation number (F) for vortex ring formation in the presence of co-flow may be defined in the same manner as Gharib *et al.* (1998). If the jet flow continues to a formation time larger than F , the leading vortex ring will stop entraining circulation and the remainder of the jet will be ejected as a trailing jet, as illustrated in §3. The formation number therefore provides a time scale for the formation of the strongest vortex ring (in terms of energy and circulation) that can be generated under the given flow conditions.

5. Formation number in co-flow

As established by Gharib *et al.* (1998), determination of the formation number requires determination of the circulation in the pinched off vortex ring. In the present investigation, pinch off was identified when the $\omega_z D / U_0 = 0.91$ iso-vorticity contour fully encircled the leading vortex ring (e.g. figure 5e). The 0.91 contour was the lowest contour level unaffected by uncertainty in the vorticity measurements (the uncertainty

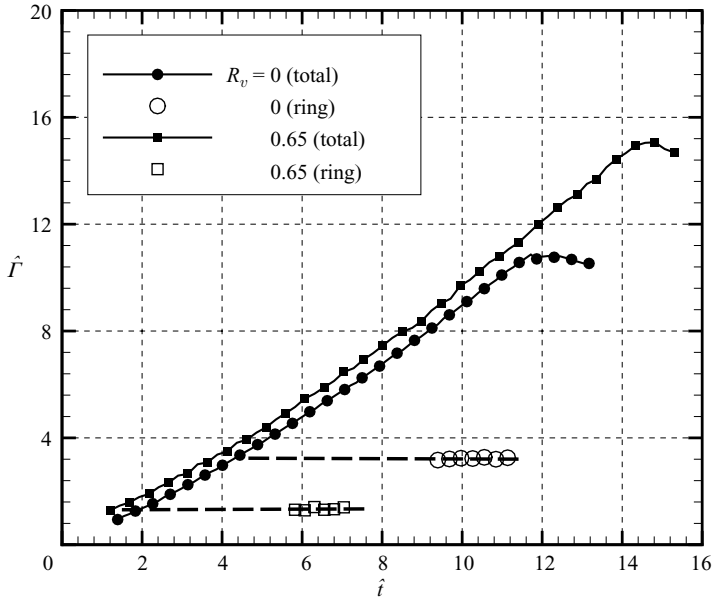


FIGURE 8. Dimensionless circulation *vs.* formation time for two cases at $\Delta\hat{t}=0$.

was $0.10(U_0/D)$, from §2), making it the best available choice for determining pinch off in the present experiment. Also, this contour level was approximately 1/5 of the peak vorticity in the pinched off vortex ring for all the $\Delta\hat{t}=0$ data (except $R_v=0$ for which it was 1/8 the peak vorticity) since the ring vorticity tended to be more diffuse at smaller R_v . Thus, the selected contour level gave a consistent treatment of pinch off across all R_v tested. More importantly, even though 1/5 the peak ring vorticity is relatively large, the 0.91 contour accurately determined the completion of the pinch off process. This was confirmed by observing that after pinch off was detected, the ring circulation was constant (to within twice the uncertainty in circulation) for more than one convective time scale D/W_r , where W_r is the ring velocity (see figure 8). Likewise, once pinch off was observed, the ring was significantly separated from the jet, as in figure 5(e), so that further entrainment of jet circulation was unlikely. These observations demonstrate that the selected contour level was able to indicate accurately when the ring had stopped entraining circulation from the generating jet and completed the formation process.

With a reliable means for determining pinch off, the formation number was determined using the protocol established by Gharib *et al.* (1998), as illustrated in figure 8 for two cases at $\Delta\hat{t}=0$. The open symbols represent the circulation of the pinched off vortex ring, that is, the circulation in the $\omega_z D/U_0=0.91$ iso-vorticity contour surrounding the ring once this contour separates from the generating jet. The filled symbols are the total circulation in the flow. (The decrease in total circulation at large \hat{t} is due to the vortex ring convecting out of the DPIV measurement frame.) The \hat{t} at which the total and ring circulations are equal for a given case is F , because the circulation supplied beyond this time is manifestly rejected by the ring. For the cases in figure 8, the results are $F \approx 4.3$ for $R_v=0$ and $F \approx 1.3$ for $R_v=0.65$.

It is worth noting that the slopes of the total circulation trends in figure 8 collapse to the same value when time is scaled as formation time (equation (4)) and circulation

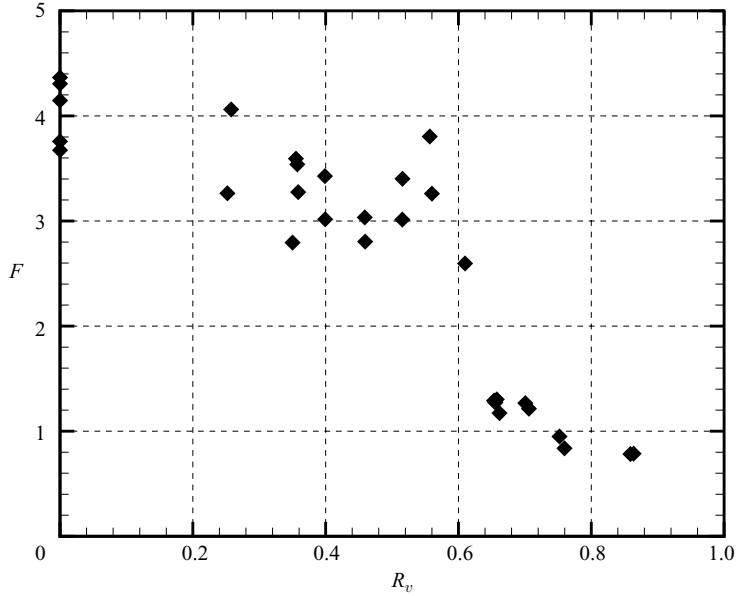


FIGURE 9. Dependence of formation number on velocity ratio for $\Delta\hat{t} = 0$.

is scaled by the strength of the jet shear layer at steady state, namely,

$$\hat{\Gamma} \equiv \frac{\Gamma}{D(U_0 - V_0)}. \quad (9)$$

This further confirms the use of equation (4) as the appropriate definition of formation time for this flow.

5.1. Formation number in simultaneously initiated co-flow ($\Delta\hat{t} = 0$)

For a given $\Delta\hat{t}$, jet velocity and shape of the velocity programs were held approximately constant, so F is expected to be a function of R_v only. The formation number for all the cases tested with simultaneously initiated co-flow ($\Delta\hat{t} = 0$) are shown in figure 9. Multiple points at the same R_v indicate multiple trials at the same nominal conditions. Error bars are excluded from figure 9 to avoid excessive clutter, but the uncertainty in an individual measurement of F is within ± 0.2 . For $R_v = 0$, $F = 4 \pm 0.5$ in agreement with the results of Gharib *et al.* (1998) for no co-flow. For $0 \leq R_v < 0.60$, the formation number drops slightly as R_v is increased, but generally stays between 3 and 4 (about a 25% variation). The circulation of the pinched off vortex ring, however, decreases by about 57% as R_v increases from 0 to 0.55. Apparently the scaling of formation time in equation (4) has somewhat compensated for the decreased circulation of the forming vortex ring, giving a formation number that is relatively insensitive to R_v for $R_v < 0.60$. The relative robustness of F for $R_v < 0.60$ is in agreement with the qualitative observations in §3 that the vortex ring formation and pinch off process is largely unaltered at small R_v .

As R_v increases beyond 0.55, F decreases sharply from approximately 3.5 to nearly 1.0 over a range in R_v that is centred around a critical velocity ratio of $R_{crit} \approx 0.60 \pm 0.05$. The decrease in F at large R_v is in agreement with Krueger *et al.* (2003). The increased R_v resolution of the present results, however, demonstrates that the drop is very sudden (but not discontinuous), being completed in a span of only 0.1 in R_v . The remarkably low F at large R_v is in agreement with the qualitative

observation that the formation process is distinctly different from the lower R_v cases, with the vortex ring pinching off almost immediately after jet initiation.

Figure 9 shows a moderate degree of variation in the results for $R_v < R_{crit}$, even at the same nominal conditions. Because of slight variations in the flow conditions (flow conditions varied slightly from the nominal conditions from trial to trial as indicated in table 1), the jet instabilities appearing behind the leading vortex ring just before pinch off would develop more rapidly in some cases. In these cases, the ring would pinch off earlier and have a slightly lower F than other cases (at the same nominal conditions) for which the jet instabilities developed more slowly. This dependence of F on trailing jet instability is in line with the observations of Zhao *et al.* (2000).

An additional parameter useful for characterizing vortex rings at pinch off is the dimensionless ring energy defined as

$$\alpha \equiv \frac{E/\rho}{\sqrt{(I/\rho)}\Gamma^3}, \quad (10)$$

where ρ is the fluid density. This parameter has been used predict the formation number based on the Kelvin–Benjamin variational principle for steadily translating vortex rings (Gharib *et al.* 1998; Mohseni & Gharib 1998; Shusser & Gharib 2000). The model predicts that a single steady vortex ring is no longer possible and the vortex ring pinches off from the jet when the generating apparatus is no longer capable of supplying energy at a rate compatible with the limiting value of α for the forming vortex ring (α_{lim}). Gharib *et al.* (1998), Zhao *et al.* (2000) and Mohseni *et al.* (2001) observed α_{lim} for pinched off vortex rings in the range 0.20 to 0.34 (the value depending somewhat on the generating conditions).

For the present experiments with co-flow, α_{lim} can be determined using the axisymmetric formulae for, E , I and Γ , namely,

$$E/\rho = \pi \int \omega \psi \, dx \, dr, \quad I/\rho = \pi \int \omega r^2 \, dx \, dr, \quad \Gamma = \int \omega \, dx \, dr, \quad (11)$$

where ψ is Stokes' streamfunction and the integration is taken over the extent of the vortex ring (i.e. the vorticity contained within the $\omega_z D/U_0 = 0.91$ iso-vorticity contour surrounding the pinched off vortex ring). As defined previously, E is the kinetic energy added to the flow, so it must be measured in the frame of reference moving with the co-flow. Explicitly,

$$E = E_L - \frac{1}{2} W_r I, \quad (12)$$

where E_L and W_r are measured in the laboratory frame.

The α_{lim} results for vortex ring formation in co-flow are shown in figure 10. The uncertainty in α_{lim} is within ± 0.015 for $R_v < 0.60$ and within ± 0.035 for $R_v > 0.60$. Clearly, the dependence of α_{lim} on R_v parallels that of F . For $R_v < R_{crit}$, α_{lim} is within the range 0.2 – 0.34. This range agrees with α_{lim} from investigations with no co-flow, so α_{lim} is relatively insensitive to co-flow for $R_v < R_{crit}$. For $R_v > R_{crit}$, α_{lim} shifts to a higher value in the range 0.47 – 0.63, characteristic of rings with smaller core radii (for example, α in the Norbury (1973) family of steady vortex rings, increases as the dimensionless core radius decreases). At the conditions tested, therefore, there are two limiting values of α . The lower value (0.2 – 0.34) occurring at low R_v , with a rapid shift to the higher value (0.47 – 0.63) promoted by increasing R_v .

5.2. Formation number for delayed initiation of co-flow ($\Delta\hat{t} > 0$)

Additional insight into the influence of co-flow on the ring formation process and on the existence of a critical velocity ratio around which F transitions to a lower value

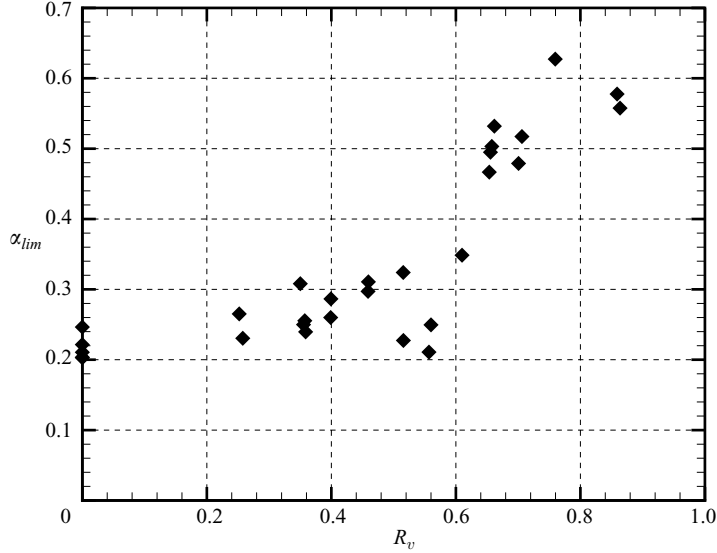


FIGURE 10. Dimensionless ring energy in the co-flow frame of reference (moving at V_0) for $\Delta\hat{t}=0$.

is achieved by delaying the initiation of the co-flow. The dependence of F on R_v for several $\Delta\hat{t} > 0$ cases is shown in figure 11. The uncertainty in the measurements of F is within ± 0.2 . The $R_v = 0$ results obtained previously are also plotted for comparison.

The general character of the results for $\Delta\hat{t} > 0$ is similar to that for $\Delta\hat{t} = 0$, namely, large F at low R_v , a rapid drop in F centred around a critical R_v , and low F at higher R_v . The magnitude of the drop in F , however, decreases with increasing $\Delta\hat{t}$. By $\Delta\hat{t} = 1.53$ (figure 11c), the drop in F has all but disappeared. The reduced magnitude of the drop in F is due primarily to larger values of F in the $R_v > R_{crit}$ range as $\Delta\hat{t}$ increases. A correlation between F at velocity ratios beyond R_{crit} and $\Delta\hat{t}$ is to be expected because the minimum F possible is $\Delta\hat{t}$ (for $\Delta\hat{t} < 4$), which is achieved if the ring pinches off the instant the co-flow is started. (For the present experiments, the minimum F achievable as $R_v \rightarrow 1$ is somewhat greater than $\Delta\hat{t}$ because the co-flow has a finite ramp-up time.) As a corollary, it is expected that for $\Delta\hat{t} > 4$, there would be no significant variation in F with R_v since the minimum possible F would be equal to the value at $R_v = 0$.

An additional distinction from the $\Delta\hat{t} = 0$ results is that the location of R_{crit} appears to decrease with increasing $\Delta\hat{t}$. From figure 11, R_{crit} is between 0.45 and 0.5 for $\Delta\hat{t} = 0.34$, at 0.4 for $\Delta\hat{t} = 0.79$, and between 0.30 and 0.35 for $\Delta\hat{t} = 1.53$ (with uncertainties of ± 0.05 in each case). Indeed, a decrease of R_{crit} from 0.6 at $\Delta\hat{t} = 0$ to between 0.45 and 0.5 for $\Delta\hat{t} = 0.34$ indicates that the critical velocity ratio is very sensitive to the startup conditions since $\Delta\hat{t} = 0.34$ corresponds to approximately twice the time required for the jet to reach its steady state value of $U_0 \approx 5.6 \text{ cm s}^{-1}$. These results suggest that the location of the sharp drop in F is directly dependent on the circulation obtained by the leading vortex during flow initiation because the circulation of the leading vortex increases with $\Delta\hat{t}$.

6. A kinematic mechanism for pinch off at $R_v > R_{crit}$

The preceding results indicate that vortex ring formation in co-flow is similar to that without co-flow (especially if the jet and co-flow are initiated simultaneously),

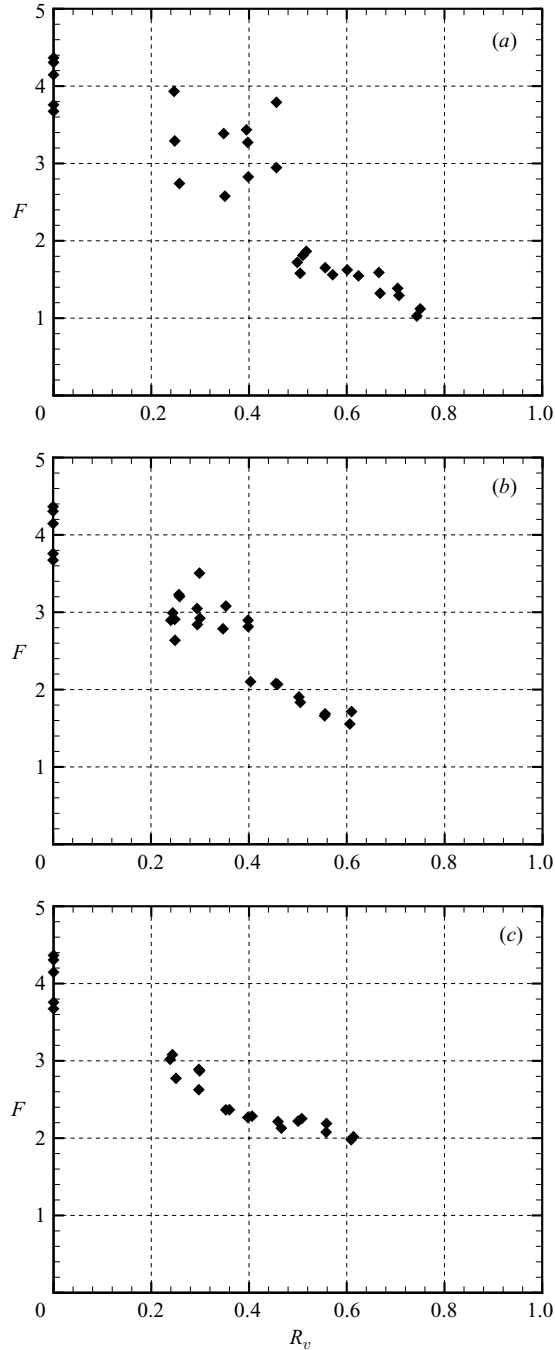


FIGURE 11. Dependence of formation number on velocity ratio for (a) $\Delta\hat{t} = 0.34 \pm 0.02$, (b) $\Delta\hat{t} = 0.79 \pm 0.02$, (c) $\Delta\hat{t} = 1.53 \pm 0.02$.

provided the velocity ratio is not too large. The behaviour at large velocity ratio is substantially different, with pinch off occurring very early (nearly as soon as the co-flow is initiated) and the circulation of the leading vortex at co-flow initiation playing a key role (as demonstrated by the $\Delta\hat{t} > 0$ results). In this section, we present

a model for pinch off at $R_v > R_{crit}$ and provide a physical explanation for the drop in F as R_v increases beyond R_{crit} .

We begin with the observation by Shusser & Gharib (2000) and Mohseni *et al.* (2001) that the ring formation process ceases and the ring pinches off once the velocity of the ring, W_r , exceeds the local velocity of the jet vorticity feeding the ring. For pinch off at $R_v > R_{crit}$, we observe that pinch off occurs very close to the nozzle and the ring is relatively weak, so the velocity of the jet vorticity in the vicinity of the ring should be approximated well by the jet shear layer velocity, namely,

$$W_s = \frac{1}{2}(U_p(t) + V_c(t)). \quad (13)$$

Then, by the above reasoning, the formation number is the formation time at which W_r first exceeds W_s . It should be noted that modelling the velocity of the jet vorticity near the ring by equation (13) is expected to work well only for $R_v > R_{crit}$. At lower velocity ratios, the vortex ring is stronger and further from the nozzle at pinch off, so the velocity of the jet vorticity near the ring can differ from equation (13) both because of the influence of the ring and because the jet centreline velocity has decayed somewhat from its value near the nozzle.

The above model can be verified by comparing W_s to the velocity of the ring determined by differentiation of the ring position. Figure 12 illustrates the comparison for two different cases with $R_v > R_{crit}$. The symbols in figure 12 represent W_r determined from measurements of the ring position. Alternatively, W_r can be determined using equation (5) where W_i for $\hat{t} > F$ is determined from a linear fit of the ring position and W_i for $\hat{t} < F$ is assumed to decrease in proportion to the ring circulation (to first order). This approximation is plotted as the bold line in figure 12 and is in excellent agreement with the velocity data determined by direct differentiation of the ring position.

Using the ring velocity determined by $W_i + V_c(t)$ as the best representation of the ring velocity (since it has the least noise), figure 12 shows that W_r exceeds W_s at a \hat{t} within ± 0.1 of F for the cases shown. In general, this model predicts F to within ± 0.2 for $R_v > R_{crit}$ in all the cases studied, verifying the model validity. A more accurate approach to determining the shear-layer velocity in the vicinity of the forming ring is to use the jet centreline velocity, u_{cl} , and co-flow velocity outside of the boundary layers, u_c , as determined from DPIV at the nozzle exit plane (see figure 4). Correcting for expansion of the jet in the vicinity of the ring (see Shusser & Gharib 2000) gives

$$W_s = \frac{1}{2} \left[\left(\frac{D}{D_r} \right)^2 u_{cl}(t) + u_c(t) \right], \quad (14)$$

where D_r is the ring diameter determined from DPIV vorticity data. Using this expression for W_s predicts the same values for F as equation (13) to within experimental uncertainty. Thus, equation (13) is sufficiently accurate for the purposes of the model.

The physical description provided by the model helps interpret the behaviour of F as R_v increases. For a significant $\Delta\hat{t}$, figure 12 (a) illustrates that pinch off is observed almost immediately after the co-flow is initiated (at $\Delta\hat{t} = 1.51$ m in this case). Clearly pinch off is initiated by the co-flow in this case. Once the co-flow has reached steady state, W_r remains substantially higher than W_s and the ring stops entraining circulation. The large disparity between W_r and W_s in figure 12 (a) is due to the relatively large W_i obtained by the ring during the jet initiation, thanks to the delayed initiation of the co-flow.

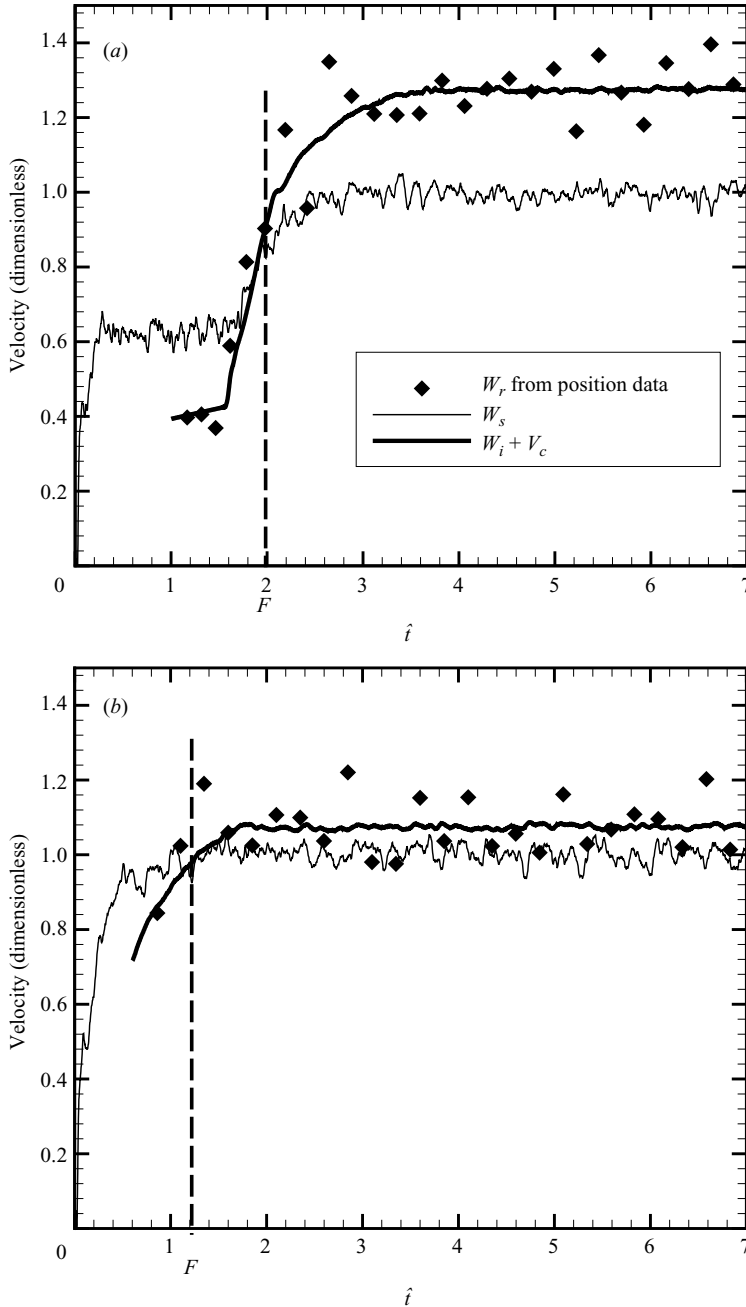


FIGURE 12. Comparison of ring and shear layer velocities for (a) $R_v = 0.61$, $\Delta \hat{t} = 1.51$, (b) $R_v = 0.71$, $\Delta \hat{t} = 0$. The formation number determined from circulation measurements is indicated by the vertical dashed lines. All velocities are normalized by $\frac{1}{2}(U_0 + V_0)$.

For $\Delta \hat{t} = 0$, the role played by the co-flow in promoting pinch off for $R_v > R_{crit}$ is less clear because the initial ring development and the co-flow initiation are not separated in time. Nevertheless, we surmise that the same mechanism is at play in figure 12(b), namely, that the forming ring pinches off under the increased convective velocity

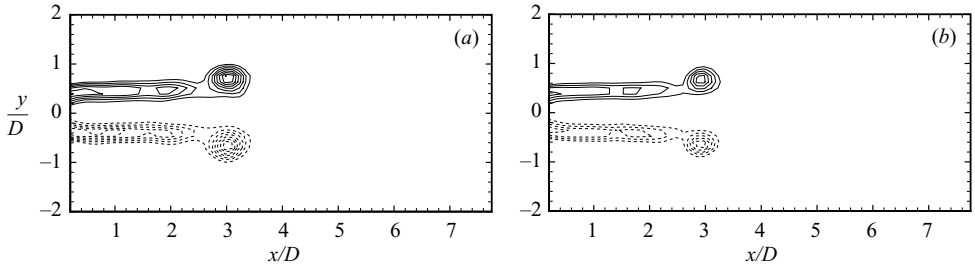


FIGURE 13. Comparison of two $\Delta\hat{t}=0$ cases at similar stages of development prior to pinch off. (a) $R_v=0.36$, $\Delta\hat{t}=6.44$, (b) $R_v=0.56$, $\Delta\hat{t}=5.88$. The contour levels are the same as in figure 5.

supplied by the co-flow as it ramps up to the steady-state value V_0 . The narrow gap between W_r and W_s is a reflection of the low circulation (low W_i) obtained by the ring before pinch off (cf. figure 7). Apparently, W_i is just large enough for the ring to pinch off early ($F \approx 1.2$) at the given level of co-flow. Significantly, the progression toward this behaviour as R_v is increased involves increasingly larger separation between the ring and the jet (before pinch off is complete) for rings at similar stages of development. This is illustrated in figure 13 for two cases ($R_v=0.36$ and 0.56 at $\Delta\hat{t}=0$). Notice that even though the leading vortex rings are at virtually the same downstream location, the separation between the peak vorticity in the ring and the nearest vorticity peak in the jet increases from $1.1D$ to $1.3D$ as R_v increases from 0.36 to 0.56 . As R_v continues to increase, eventually the separation between the ring and the jet is so large that the ring is only able to entrain circulation at the initial stages of ring formation and the ring pinches off from the jet at a much earlier stage than observed at lower R_v . The model indicates that a major factor leading to the increased separation between the ring and the jet is the larger convective velocity provided to the ring at higher R_v . Entrainment of vorticity into the instability peak that develops at the leading edge of the trailing-jet further enhances the separation and promotes completion of the pinch off process (Zhao *et al.* 2000). The trailing-jet instability plays a diminishing role, however, as R_v is increased and the instability is suppressed (which accounts for the low degree of variability in F for $R_v > R_{crit}$).

In addition to elucidating the pinch off behaviour at large R_v , the model also explains the reduction in R_{crit} as $\Delta\hat{t}$ increases. For larger $\Delta\hat{t}$, W_i is larger at the initiation of co-flow. Thus, W_r is larger for a given R_v and the conditions required to promote a substantial reduction in the formation number are achieved at a lower R_v . For $\Delta\hat{t}=0$, the W_i obtained by the initial development of the ring (i.e. the ring development before the co-flow reaches V_0) is determined by $U_p(t) - V_c(t)$ during flow initiation. As described earlier, the ramp-up for $U_p(t)$ was much more rapid than that for $V_c(t)$ and it was impossible to maintain a constant $V_c(t)/U_p(t)$ during flow initiation with the present apparatus. By implication, the value of $R_{crit} \approx 0.60$ observed in the results for $\Delta\hat{t}=0$ may be somewhat dependent on the apparatus itself. Indeed, it may be possible to achieve a formation number in the range 3 to 4 over a greater R_v range, allowing R_{crit} to approach 1, if the flow initiation were properly tailored to maintain $V_c(t)/U_p(t) = V_0/U_0 = \text{constant}$ throughout. The effect of increasing R_v would then be to delay the completion of vortex ring pinch off to a point further downstream and to increase the likelihood that any miscue in the flow initiation process would lead to a drop in F .

7. Concluding remarks

The behaviour of vortex ring formation and pinch off from an impulsively started jet with uniform background co-flow was investigated. The present study confirms the results of the brief study by Krueger *et al.* (2003), indicating that a dramatic shift takes place in the formation process when R_v is sufficiently high. This shift is characterized by a drop in F over a very short range in R_v , a much lower ring circulation at pinch off, and completion of vortex ring pinch off very close to the jet nozzle. Complementary behaviour is observed for the limiting dimensionless ring energy at pinch off, α_{lim} , where α_{lim} is in the range 0.20–0.34 for low R_v and suddenly shifts to a higher value in the range 0.47–0.63 as R_v is increased. Delaying co-flow initiation shifted the R_v at the center of the drop in F (R_{crit}) to lower values and decreased the magnitude of the drop because the circulation of the leading vortex ring was larger in these cases. A kinematic model was proposed and found to predict the pinch off process accurately for $R_v > R_{crit}$. The results demonstrated that at sufficiently high R_v , the vortex ring formation process was pre-empted by the increased ring velocity as a result of convection from the co-flow.

The tendency for sufficiently large co-flow to pre-empt ring formation is consistent with methods of manipulating the F discussed in previous studies. Mohseni *et al.* (2001) demonstrated pinch off could be delayed and F increased if the jet velocity were increased during formation so that the shear layer could keep pace with the forming ring. Likewise, Dabiri & Gharib (2004) demonstrated that counterflow (or negative co-flow) could increase F by retarding the ring velocity and maintaining the ring proximity to the jet. The present results seem to be the inverse of these examples, with the ring being more rapidly separated from the jet by the co-flow, thereby hampering the formation process. Nevertheless, the sensitivity of vortex ring formation and pinch off to co-flow, manifested as a sharp drop in F , seems to be a unique feature of the current investigation (i.e. the cases where F has been increased did not show a sudden increase in F as the parameters were varied). The rapid reduction in F over a short range in R_v presents a significant limitation for situations where vortex ring formation is a key feature of the flow, such as pulsed jet propulsion. Furthermore, the significant role played by the initial ring formation on the location and magnitude of the drop in F (demonstrated by the results for delayed initiation of co-flow) shows that the prescribed velocity program is a key factor influencing vortex ring formation in the presence of co-flow. This indicates the need to consider realistic velocity programs (both for the jet and co-flow) in evaluating the mechanics of starting jets in applications such as propulsion and hints at the possibility that nature may tailor the velocity programs to achieve performance gains in natural instances of starting jet flows.

REFERENCES

- DABIRI, J. O., COLIN, S. P., COSTELLO, J. H. & GHARIB, M. 2005 Flow patterns generated by oblate medusan jellyfish: field measurements and laboratory analyses. *J. Exp. Biol.* **208**, 1257–1265.
- DABIRI, J. O. & GHARIB, M. 2004 Delay of vortex ring pinchoff by an imposed bulk counterflow. *Phys. Fluids* **16**, L28–L30.
- DIDDEN, N. 1979 On the formation of vortex rings: rolling-up and production of circulation. *Z. Angew. Math. Phys.* **30**, 101–116.
- GHARIB, M., RAMBOD, E. & SHARIFF, K. 1998 A universal time scale for vortex ring formation. *J. Fluid Mech.* **360**, 121–140.
- KRUEGER, P. S. 2001 The significance of vortex ring formation and nozzle exit over-pressure to pulsatile jet propulsion. PhD thesis, California Institute of Technology.

- KRUEGER, P. S. 2005 An over-pressure correction to the slug model for vortex ring circulation. *J. Fluid Mech.* **545**, 427–443.
- KRUEGER, P. S. & GHARIB, M. 2003 The significance of vortex ring formation to the impulse and thrust of a starting jet. *Phys. Fluids* **15**, 1271–1281.
- KRUEGER, P. S., DABIRI, J. O. & GHARIB, M. 2003 Vortex ring pinch-off in the presence of simultaneously initiated uniform background co-flow. *Phys. Fluids* **15**, L49–L52.
- LINDEN, P. F. & TURNER, J. S. 2001 The formation of ‘optimal’ vortex rings, and the efficiency of propulsion devices. *J. Fluid Mech.* **427**, 61–72.
- MADIN, L. P. 1990 Aspects of Jet Propulsion in Salps. *Can. J. Zool.* **68**, 765–777.
- MOHSENI, K. & GHARIB, M. 1998 A model for universal time scale of vortex ring formation. *Phys. Fluids* **10**, 2436–2438.
- MOHSENI, K., RAN, H. & COLONIUS, T. 2001 Numerical experiments on vortex ring formation. *J. Fluid Mech.* **430**, 267–282.
- NORBURY, J. 1973 A family of steady vortex rings. *J. Fluid Mech.* **57**, 417–443.
- ROSENFELD, M., RAMBOD, E. & GHARIB, M. 1998 Circulation and formation number of laminar vortex rings. *J. Fluid Mech.* **376**, 297–318.
- SHARIFF, K. & LEONARD, A. 1992 Vortex rings. *Annu. Rev. Fluid Mech.* **24**, 235–279.
- SHUSSER, M. & GHARIB, M. 2000 Energy and velocity of a forming vortex ring. *Phys. Fluids* **12**, 618–621.
- WESTERWEEL, J., DABIRI, D. & GHARIB, M. 1997 The effect of a discrete window offset on the accuracy of cross-correlation analysis of digital PIV recordings. *Exps. Fluids* **23**, 20–28.
- WILLERT, C. E. & GHARIB, M. 1991 Digital particle image velocimetry. *Exps. Fluids* **10**, 181–193.
- ZHAO, W., FRANKEL S. H. & MONGEAU, L. G. 2000 Effects of trailing jet instability on vortex ring formation. *Phys. Fluids* **12**, 589–596.